Published in final edited form as:
Cell Tissue Res. 2008 September ; 333(3): 395–403. doi:10.1007/s00441-008-0641-5.

Cellular characterization of Connexin26 and Connnexin30 expression in the cochlear lateral wall

Ying-Peng Liu and **Hong-Bo Zhao**
Department of Surgery - Otolaryngology, University of Kentucky Medical Center, 800 Rose Street, Lexington KY 40536-0293, USA, e-mail: hzhao2@uky.edu

Abstract

Gap junctions in the cochlear lateral wall, which consists of the stria vascularis (SV) and spiral ligament (SPL), are important for generating a positive endocochlear potential and high potassium concentration in the endolymph. In this study, the cellular expression of connexin 26 (Cx26) and Cx30 in the cochlear lateral wall of rats and guinea pigs was examined by immunofluorescent staining and confocal microscopy. Co-labeling for Kir4.1 revealed that the stria intermediate cells had extensive labeling for Cx26 and Cx30 with a leaf-like distribution. Cx26 and Cx30 also co-distributed hexagonally around the basal cells. However, no labeling was observed in the marginal cells. In the SPL, punctate Cx26 and Cx30 labeling was distributed along vertical lines orthogonal to the cochlear longitudinal direction. Intense labeling for Cx26 and Cx30 was found in type II fibrocytes in the spiral prominence and central region, but Cx26 labeling was absent in the middle region just beneath the SV, where only Cx30 labeling was observed. Outer sulcus (OS) cells and their root processes also exhibited intense labeling for Cx26 and Cx30. Neither Cx26 nor Cx30 was immunopositive in the hyaline region beneath the OS, in the subcentral region (type IV fibrocytes), or in the tension (type III) fibrocytes beneath the bone. Cx26 and Cx30 labeling was also absent in the lateral wall blood vessels. Thus, Cx26 and Cx30 have distinct cell-specific distributions in the SV and SPL, suggesting that they can form different pathways for transporting ions/nutrients in the cochlear lateral wall.

Keywords

Gap junction; Connexin; Kir4.1; Stria vascularis; Spiral ligament; Inner ear; Non-syndromic hearing loss; Guinea pig; Rat

Introduction

A gap junctional channel is an intercellular channel that forms an intracellular conduit for direct electrical and metabolic communication between cells. This intercellular communication plays a crucial role in hearing. Mutations in the gap junction gene *connexin* have been reported to induce a high incidence of nonsyndromic hearing loss (Kelsell et al. 1997). Gap junctional coupling extensively exists in the cochlear tissues (for a review, see Zhao et al. 2006). Two independent gap junctional networks have been identified: the epithelial gap junctional network between supporting cells in the auditory sensory epithelium in the organ of Corti and the connective tissue gap junctional network between the connective tissue cells in the cochlear lateral wall (Kikuchi et al. 1995).

Correspondence to: Hong-Bo Zhao.

The cochlear lateral wall is composed of the stria vascularis (SV) and spiral ligament (SPL), responsible for the generation and maintenance of the high positive endocochlear potential (EP, +80 mV) and high K^+ concentration (155 mM) in the cochlear endolymph. This is a driving force for hair cells to produce the auditory receptor current. Gap-junction-mediated intercellular communication has been hypothesized to play a crucial role in this driving force generation and maintenance (for reviews, see Couloigner et al. 2006; Wangemann 2006; Zhao et al. 2006). During development, the onset and growth of EP is reported to be associated with the establishment of intercellular communication and connexin expression in the cochlear lateral wall (Souter and Forge 1998; Lautermann et al. 1999; Xia et al. 1999; Suzuki et al. 2001; Lopez-Bigas et al. 2002). Genetic mutation studies have also demonstrated that intercellular communication in the cochlear lateral wall is required for EP generation (Steel et al. 1987; Steel and Barkway 1989; Carlisle et al. 1990).

Connexin 26 (Cx26) and Cx30 are predominant isoforms in the cochlea and are prevalently expressed in both the epithelial gap junctional network and the connective tissue gap junctional network (Kikuchi et al. 1995; Lautermann et al. 1998, 1999; Forge et al. 1999, 2003; Zhao and Yu 2006). In the epithelial gap junctional network, Cx26 and Cx30 have been found to have cell-specific distributions in the cochlear sensory epithelium (Zhao and Yu 2006). Functional studies have revealed that Cx26 and Cx30 have strong charge selectivity in permeability (Zhao 2005); Cx26 is mainly responsible for anionic permeability in the cochlear sensory epithelium and plays an important role in the intercellular signaling (Zhao 2005; Zhao et al. 2005).

In this study, we have systematically investigated the cellular characteristics of Cx26 and Cx30 expression in the cochlear lateral wall. We have found that Cx26 and Cx30 have distinct cell-specific distributions in the SV and SPL. These results provide important morphogenetic clues for further study of the putative function(s) of Cx26 and Cx30 in the cochlear lateral wall for hearing.

Preliminary data from this study have been presented at a meeting in abstract form (Liu and Zhao 2007).

Materials and methods

Animal preparation and cochlear lateral wall dissociation

A total of 16 adult Hartley guinea pigs and 11 adult rats were used. Animal preparation has been reported elsewhere (Zhao 2005; Zhao and Yu 2006). Briefly, animals were anesthetized with pentobarbital and then decapitated. The temporal bone was removed and dissected in a standard extracellular solution (142 mM NaCl, 5.37 mM KCl, 1.47 mM $MgCl_2$, 2 mM $CaCl_2$, 10 mM HEPES, 300 mOsm, pH 7.2). After removal of the lateral bone, the cochlear lateral wall was exposed and then torn off by forceps (Fig. 1a). The SV was further separated from the SPL by micro-dissection (Fig. 1b). In the dissociated cell preparation, the SV and SPL strips were enzymed separately by trypsin (1–5 mg/ml) with shaking for 5–10 min. After the residual enzyme had been washed out by the extracellular solution, the dissociated cells were transferred to dishes for staining. All experimental procedures were approved by the University of Kentucky's Animal Care & Use Committee and conducted according to the standards of the NIH Guidelines for the Care and Use of Laboratory Animals.

Preparation of cochlear cross sections

The isolated cochlea was fixed with 4% paraformaldehyde for 30 min and then decalcified in 10% EDTA at room temperature with gentle agitation for 4–6 days (Hurley et al. 2003). The solution was changed every day. The decalcified cochlea was further infiltrated with 30% glucose for 2 days and then embedded in 15% gelatin with 2.5% glycerol at 37°C, with gentle

suction on the round window of the cochlea to permit the gelatin to fill the cochlea completely. The embedded cochlea was maintained at room temperature for 1 h to allow solidification of the gelatin and subsequently cut at a thickness of 15 μm at −22to −24°C on a cryostat (Thermo Electron, Waltham, Mass.). The tissue sections were collected and mounted onto glass slides for staining and storage.

Immunofluorescent staining

Immunofluorescent staining was performed as previously reported (Zhao and Yu 2006). The separated SV and SPL strips or dissociated cells were fixed with 4% paraformaldehyde for 30 min. After being washed three times with 0.1 M phosphate-buffered saline (PBS), the tissues or cells were incubated in a blocking solution (10% goat serum and 1% bovine serum albumin in PBS) with 0.1% Triton X-100 for 20 min. Then, the tissues or cells were incubated with a mixture of anti-Cx26 and anti-Cx30 antibodies (1:400; cat. no. 33–5800 and 71–2200, respectively, Zymed Laboratories, South San Francisco, Calif.) in the blocking solution at 4° C overnight. After being washed three times with 0.1 M PBS, the tissues or cells were reacted with a mixture of Alexa Fluor 488-conjugated goat anti-mouse IgG and Alexa Fluor 568-conjugated goat anti-rabbit IgG (1:500; cat. no. A11029 and A11036, respectively, Molecular Probes) in the blocking solution at room temperature for 1 h. For Kir4.1 labeling, an affinity-purified goat polyclonal anti-Kir4.1 antibody (1:100; cat. no. sc-23637; Santa Cruz Biotech, Santa Cruz, Calif.) and donkey anti-goat Alexa Fluor 568 (1:500; cat. no. A11057, Molecular Probes) were used. After the secondary antibodies had been completely washed out with 0.1 M PBS, the tissues or cells were observed under a confocal laser-scanning microscope. The hair cells and marginal cells that had no gap junctional coupling and connexin expressions served as an internal negative control. We also omitted the primary antibodies as a negative control. No immunofluorescent labeling was observed.

In some cases, cell nuclei were also visualized by staining with 4′,6-diamidino-2-phenylindole (DAPI, 0.1 mg/ml; D1306; Molecular Probes) for 15–20 min at room temperature, following the 2nd antibody incubation.

Confocal microscopy and image presentation

The stained tissues or cells were observed under a Leica confocal microscope (Leica TCS SP2) equipped with 40× (N/A: 1.25) and 100× (N/A: 1.4) apochromatic oil objectives. An argon laser (488 nm) and krypton laser (568 nm) with 500–530 nm and 600–665 nm emission filters were used to visualize Alexa Fluor 488 and 568, respectively, by sequentially scanning. DAPI staining was visualized by a two-photon laser with a 388–478 nm emission filter. The fluorescent image was saved in the TIFF format and assembled in Photoshop (Adobe Systems, Mountain View, Calif.) for presentation. Serial confocal sections were also reconstructed by Image-Pro Plus (Media Cybernetics, Bethesda, Md.) for three-dimensional (3D) views.

Results

Cellular expression of Cx26 and Cx30 in SV

The SV is composed of three cell layers, i.e., the marginal cell layer, intermediate cell layer, and basal cell layer (Fig. 1c). At the basal cell layer, Cx26 and Cx30 showed intense punctate labeling surrounding the basal cells, demonstrating a hexagonal distribution pattern (Fig. 2). The puncta of Cx26 and Cx30 labeling largely overlapped and could be located in the same gap junctional plaques (Fig. 2c). Kir4.1 has previously been found to be expressed exclusively in the intermediate cells in the SV (Ando and Takeuchi 1999). In double-immunofluorescent labeling for Cx26 and Kir4.1, the Cx26 labeling appeared in a honeycomb-like distribution pattern, whereas labeling for Kir4.1 was negative (Fig. 2e). This confirmed that the recorded

honeycomb-like labeling pattern was located in the basal cell layer, rather than in the neighboring intermediate cell layer.

The stria intermediate cells also showed strongly positive labeling for Cx26 and Cx30 (Fig. 3a–g). However, the labeling pattern was different from that observed in the basal cell layer, appearing to be irregular and leaf-like (Fig. 3a–c). The puncta of Cx26 and Cx30 labeling were large and also present at the cell edge on the non-junctional cell surface (white arrows in Fig. 3c). The labeling for Kir4.1 was positive (Fig. 3e) but did not overlap with the Cx26 labeling on the cell surface (Fig. 3f). Nomarski imaging revealed the dendrite-like projections and cytoplasmic pigment granules (arrows in Fig. 3g) of the intermediate cells. Marginal cells were also large (Fig. 3h) but exhibited no labeling for Cx26 and Cx30 (Fig. 3i–j). The marginal cells also showed negative labeling for Kir4.1 (data not shown).

Distributions of Cx26 and Cx30 in SPL

Unlike the distribution of Cx26 and Cx30 in the SV, Cx26 and Cx30 labeling in the SPL was distributed along the dorsal-ventral line orthogonal to the longitudinal direction of the SPL (Fig. 4a–c). The labeling appeared slightly less intense in the middle region at the SV location (note that the SV had been removed from the SPL before staining). Whereas the puncta of Cx26 and Cx30 co-labeling were visible (Fig. 4c–d), Cx26 and Cx30 had different distribution patterns in the SPL. In serial confocal scanning sections, Cx26 labeling was intense at the edge region of the SPL but less intense in the middle region in the sections near the SV (Fig. 5a–d). On scanning toward the outer surface (the bone-face), Cx26 labeling became intense and visible in the middle region (Fig. 5e–i). Cx30 showed intense labeling in the middle region just beneath the SV and overlapped with Cx26 expression near the outer surface (Fig. 5a–l). The blood vessels were also visible in the middle serially scanned sections but had no Cx26 and Cx30 labeling (white arrows in Fig. 5f–h).

We reconstructed 3D images from serial scanning sections (Fig. 5n–o). At the reconstructed orthogonal cross-cochlear plane (Fig. 5o), Cx26 labeling was intense at the apical tip of the SPL but weak or even absent in the middle region just beneath the SV (asterisk in Fig. 5o), where the Cx30 labeling was intense. The same distribution pattern was observed in a total of 12 observations in two guinea pigs and three rats.

Consistent with observations in the reconstructed 3D images in whole-mount preparations, Cx26 in the cochlear cross-sectional preparation showed intense labeling at the apical tip of the SPL and the spiral prominence (SP; Fig. 6a–c). In the orthogonal midmodiolar cross section through the cochlear diameter (Fig. 6a, e–f), Cx26 labeling was observed in the outer peripheral region in the middle SPL but was absent in the subregion just beneath the SV. Intense Cx26 and Cx30 labeling was also observed in the outer sulcus (OS) cells and their root processes (white arrows and open arrowhead, respectively, in Fig. 6g). However, the labeling for Cx26 and Cx30 was absent in the tension (type III) fibrocytes area behind the otic capsule, the subcentral region (asterisks in Fig. 6a–d, g–h), and the hyaline region just beneath the OS within the basilar crest (Fig. 6h).

Discussion

In this study, we have demonstrated that Cx26 and Cx30 have distinct cellular distributions in the SV and SPL in the cochlear lateral wall (Fig. 7). By co-labeling for Kir4.1, we have found that Cx26 and Cx30 exhibit intense labeling in the stria intermediate cells (Fig. 3a–g). Unlike the honeycomb-like distribution of Cx26 and Cx30 in the basal cells, however, Cx26 and Cx30 labeling in the intermediate cells appears with a leaf-like pattern. However, neither Cx26 nor Cx30 are immunopositive in marginal cells (Fig. 3h–j). In the SPL, Cx26 immunostaining is intense in type V fibrocytes at the apical tip of the SPL, but this is less intense in the middle

region just beneath the SV, where Cx30 shows intense labeling (Figs. 5, 6). Immunofluorescent labeling for Cx26 and Cx30 is also intense in the type II fibrocytes in the SP and central region, and in the OS cells and their root processes (Figs. 5, 6). However, no labeling for Cx26 and Cx30 has been observed in the type IV fibrocytes in the subcentral region inferior to the basilar membrane near the scala tympani, the type III (tension) fibrocytes area beneath the otic capsule, or the hyaline region beneath the OS cells (Figs. 5, 6). Cx26 and Cx30 also show negative labeling in the blood vessels in the lateral wall (Fig. 5f–h).

In the cochlea, the SV is responsible for the generation of the uniquely high positive EP and high potassium concentration in the endolymph. According to the proposed model (Salt et al. 1987; Takeuchi et al. 2000; Marcus et al. 2002), the intermediate cell in the SV plays a critical role in positive EP generation. Gap junctional coupling between the intermediate cells and the basal cells is required for this mechanism (Steel et al. 1987; Steel and Barkway 1989; Carlisle et al. 1990). However, little information on gap junctional coupling and connexin expression in the intermediate cell is available. In this study, by co-staining for Kir4.1, we have unambiguously identified the expression and distribution of Cx26 and Cx30 in the intermediate cells (Fig. 3a–g). This provides direct evidence for the existence of connexin expression in the intermediate cells.

Moreover, we have further demonstrated the pattern of distribution of Cx26 and Cx30 expression in the intermediate cells; Cx26 and Cx30 labeling appears to be extensive and leaf-like and is distributed on the surface of the intermediate cells (Fig. 3a–g). In vivo, the apical membrane of the intermediate cell faces the intrastrial space and is not directly in contact with the marginal cell (see Fig. 1c). Cx26 and Cx30 expression on this unconnected apical cell surface may allow them to act as functional hemichannels. The intrastrial space is characterized by a high positive potential (+90 mV) and a low Ca^{++} concentration (0.8 mM; Wangemann 2006). This electrochemical environment favors hemichannel opening (Goodenough and Paul 2003). We have reported that hemichannels in the cochlear sensory epithelium can open to release ATP to modify outer hair cell electromotility (Zhao et al. 2005). Cx26 and Cx30 may also function as hemichannels on the intermediate cell surface at the intrastrial space and may have a function in the generation of EP and high K^+ concentration in the endolymph.

In this study, we have also found intense co-labeling for Cx26 and Cx30 hexagonally around the basal cells (Fig. 2). In vivo, the basal cells connect with intermediate cells in the SV and fibrocytes in the SPL (Fig. 1e). In the middle region, the fibrocytes in the SPL beneath the basal cells only exhibit Cx30 labeling (Figs. 5, 6). This implies that Cx30 and Cx26 form heterotypic and/or heteromeric gap junctional channels in this SV-SPL interface, in addition to Cx30 homotypic channels. We have previously reported that Cx26 and Cx30 in the cochlear supporting cells can form functional hybrid (heterotypic/heteromeric) channels with asymmetric voltage gating (Zhao and Santos-Sacchi 2000) that can induce asymmetric transjunctional transfer in the cochlear sensory epithelium (Zhao 2000) and that may play an important role in directional intercellular transport, such as the proposed K^+-recycling in the cochlear sensory epithelium (Kikuchi et al. 1995;Zhao 2000,2003). In the cochlear lateral wall, K^+ ions have been postulated to be directionally transported from the SPL to the SV to be secreted into the endolymph for generation of the EP and K^+-gradient (Kikuchi et al. 1995;Spicer and Schulte 1998;Zhao et al. 2006). Indeed, mutant studies have demonstrated that some deafness-linked Cx26 mutants (e.g., mutations of V84L, V95M, and E114G) specifically impair heterotypic channel formation and function to induce hearing loss (Choung et al. 2002;Thonnissen et al. 2002;Bruzzone et al. 2003;Wang et al. 2003).

Unlike the connexin distributions in the SV cells, the connexin-labeled puncta in the SPL are distributed along dorsal-ventral vertical lines (Figs. 4, 5). This implies that fibrocytes may have good coupling and intercellular communication in the longitudinal direction in the SPL. As

shown in Figs. 5, 6, Cx30 labeling is widely distributed in the SPL, whereas Cx26 labeling is intense in type V fibrocytes at the apical tip of the SPL, type I fibrocytes at the outer peripheral region, and type II fibrocytes in the SP and central region (Figs. 5, 6, 7). These fibrocytes have been proposed to form different pathways for K^+-recycling (Spicer and Schulte 1998). Interestingly, the OS cells and their root processes exhibit intense labeling for Cx30 and Cx26 (Fig. 6g, h). However, the hyaline region beneath the OS cells lacks Cx26 and Cx30 labeling. This suggests that OS cells and their root processes can form a transport pathway in the SPL for ionic transfer. It also provides direct histological evidence that the OS cells can participate in K^+-transport to maintain and regulate the endolymphatic K^+ concentration (Marcus and Chiba 1999).

In this study, we have demonstrated that Cx26 and Cx30 have distinct cell-specific distributions in the guinea pig and rat cochlear lateral wall. These Cx26 and Cx30 cell-specific distributions provide morphological evidence that Cx26 and Cx30 can play different roles in the transport of ions/nutrients in the cochlear lateral wall.

Acknowledgements

This work was supported by NIDCD DC 05989.

We thank Mary G. Engle for technical support with the confocal microscopy.

References

Ando M, Takeuchi S. Immunological identification of an inward rectifier K^+ channel (Kir4.1) in the intermediate cell (melanocyte) of the cochlear stria vascularis of gerbils and rats. Cell Tissue Res 1999;298:179–183. [PubMed: 10555552]

Bruzzone R, Veronesi V, Gomes D, Bicego M, Duval N, Marlin S, Petit C, D'Andrea P, White TW. Loss-of-function and residual channel activity of connexin26 mutations associated with non-syndromic deafness. FEBS Lett 2003;533:79–88. [PubMed: 12505163]

Carlisle L, Steel K, Forge A. Endocochlear potential generation is associated with intercellular communication in the stria vascularis: structural analysis in the viable dominant spotting mouse mutant. Cell Tissue Res 1990;262:329–337. [PubMed: 2076537]

Choung YH, Moon SK, Park HJ. Functional study of GJB2 in hereditary hearing loss. Laryngoscope 2002;112:1667–1671. [PubMed: 12352684]

Couloigner V, Sterkers O, Ferrary E. What's new in ion transports in the cochlea? Pflugers Arch 2006;453:11–22. [PubMed: 16773381]

Forge A, Becker D, Casalotti S, Edwards J, Evans WH, Lench N, Souter M. Gap junctions and connexin expression in the inner ear. Novartis Found Symp 1999;219:134–163. [PubMed: 10207902]

Forge A, Becker D, Casalotti S, Edwards J, Marziano N, Nevill G. Gap junctions in the inner ear: comparison of distribution patterns in different vertebrates and assessement of connexin composition in mammals. J Comp Neurol 2003;467:207–231. [PubMed: 14595769]

Goodenough DA, Paul DL. Beyond the gap: functions of unpaired connexon channels. Nat Rev Mol Cell Biol 2003;4:284–294.

Hurley PA, Clarke M, Crook JM, Wise AK, Shepherd RK. Cochlear immunochemistry—a new technique based on gelatin embedding. J Neurosci Methods 2003;129:81–86. [PubMed: 12951235]

Kelsell DP, Dunlop J, Stevens HP, Lench NJ, Liang JN, Parry G, Mueller RF, Leigh IM. Connexin 26 mutations in hereditary nonsyndromic sensorineural deafness. Nature 1997;387:80–83. [PubMed: 9139825]

Kikuchi T, Kimura RS, Paul DL, Adams JC. Gap junctions in the rat cochlea: immunohistochemical and ultrastructural analysis. Anat Embryol 1995;191:101–118. [PubMed: 7726389]

Lautermann J, Cate WJ ten, Altenhoff P, Grummer R, Traub O, Frank H, Jahnke K, Winterhager E. Expression of the gap-junction connexins 26 and 30 in the rat cochlea. Cell Tissue Res 1998;294:415–420. [PubMed: 9799458]

Lautermann J, Frank HG, Jahnke K, Traub O, Winterhager E. Developmental expression patterns of connexin26 and –30 in the rat cochlea. Dev Genet 1999;25:306–311. [PubMed: 10570462]

Liu, YP.; Zhao, HB. Quantitative analysis of connexin26 and connexin30 expressions in the lateral wall of the mammalian cochlea. The 30th assoc res otolaryngol annual meeting; Denver, Colo.. 10–15 Feb 2007; 2007. (http://www.aro.org)

Lopez-Bigas N, Arbones ML, Estivill X, Simonneau L. Expression profiles of the connexin genes, Gjb1 and Gjb3, in the developing mouse cochlea. Gene Expr Patterns 2002;2:113–117. [PubMed: 12617848]

Marcus DC, Chiba T. K^+ and Na^+ absorption by outer sulcus epithelial cells. Hear Res 1999;134:48–56. [PubMed: 10452375]

Marcus DC, Wu T, Wangemann P, Kofuji P. KCNJ10 (Kir4.1) potassium channel knockout abolishes endocochlear potential. Am J Physiol Cell Physiol 2002;282:C403–C407. [PubMed: 11788352]

Salt AN, Melichar I, Thalmann R. Mechanisms of endocochlear potential generation by stria vascularis. Laryngoscope 1987;97:984–991. [PubMed: 3613802]

Souter M, Forge A. Intercellular junctional maturation in the stria vascularis: possible association with onset and rise of endocochlear potential. Hear Res 1998;119:81–95. [PubMed: 9641321]

Spicer SS, Schulte BA. Evidence for a medial K^+ recycling pathway from inner hair cells. Hear Res 1998;118:1–12. [PubMed: 9606057]

Steel KP, Barkway C. Another role for melanocytes: their importance for normal stria vascularis development in the mammalian inner ear. Development 1989;107:453–463. [PubMed: 2612372]

Steel KP, Barkway C, Bock GR. Strial dysfunction in mice with cochleo-saccular abnormalities. Hear Res 1987;27:11–26. [PubMed: 3583934]

Suzuki T, Oyamada M, Takamatsu T. Different regulation of connexin26 and ZO-1 in cochleas of developing rats and of guinea pigs with endolymphatic hydrops. J Histochem Cytochem 2001;49:573–586. [PubMed: 11304795]

Takeuchi S, Ando M, Kakigi A. Mechanism generating endocochlear potential: role played by intermediate cells in stria vascularis. Biophys J 2000;79:2572–2582. [PubMed: 11053131]

Thonnissen E, Rabionet R, Arbones ML, Estivill X, Willecke K, Ott T. Human connexin26 (GJB2) deafness mutations affect the function of gap junction channels at different levels of protein expression. Hum Genet 2002;111:190–197. [PubMed: 12189493]

Wang HL, Chang WT, Li AH, Yeh TH, Wu CY, Chen MS, Huang PC. Functional analysis of connexin-26 mutants associated with hereditary recessive deafness. J Neurochem 2003;84:735–742. [PubMed: 12562518]

Wangemann P. Supporting sensory transduction: cochlear fluid homeostasis and the endocochlear potential. J Physiol (Lond) 2006;576:11–21. [PubMed: 16857713]

Xia A, Kikuchi T, Hozawa K, Katori Y, Takasaka T. Expression of connexin 26 and Na, K-ATPase in the developing mouse cochlear lateral wall: functional implications. Brain Res 1999;846:106–111. [PubMed: 10536217]

Zhao HB. Directional rectification of gap junctional voltage gating between Deiters cells in the inner ear of guinea pig. Neurosci Lett 2000;296:105–108. [PubMed: 11108992]

Zhao, HB. Biophysical properties and functional analysis of inner ear gap junctions for deafness mechanisms of nonsyndromic hearing loss. Proceedings of the 9th international meeting on gap junctions; Cambridge, United Kingdom. 23–28 August 2003; 2003.

Zhao HB. Connexin26 is responsible for anionic molecule permeability in the cochlea for intercellular signalling and metabolic communications. Eur J Neurosci 2005;21:1859–1868. [PubMed: 15869481]

Zhao HB, Santos-Sacchi J. Voltage gating of gap junctions in cochlear supporting cells: evidence for nonhomotypic channels. J Memb Biol 2000;175:17–24.

Zhao HB, Yu N. Distinct and gradient distributions of connexin26 and connexin30 in the cochlear sensory epithelium of guinea pigs. J Comp Neurol 2006;499:506–518. [PubMed: 16998915]

Zhao HB, Yu N, Fleming CR. Gap junctional hemichannel-mediated ATP release and hearing controls in the inner ear. Proc Natl Acad Sci USA 2005;102:18724–18729. [PubMed: 16344488]

Zhao HB, Kikuchi T, Ngezahayo A, White TW. Gap junctions and cochlear homeostasis. J Memb Biol 2006;209:177–186.

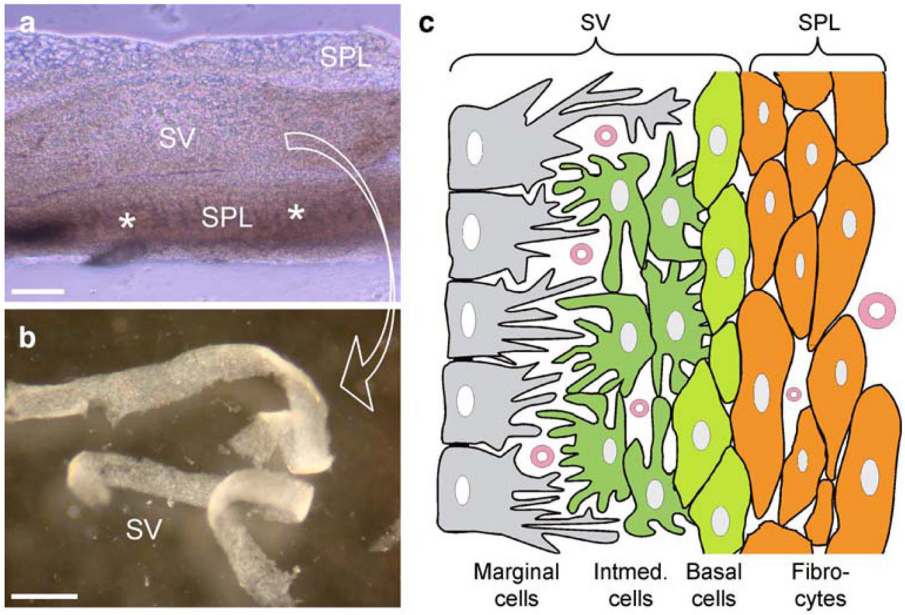

Fig. 1.

Structure of the cochlear lateral wall. **a** Isolated cochlear lateral wall (*asterisks* spiral prominence and the inferior region below the spiral prominence, *SV* stria vascularis, *SPL* spiral ligament). **b** The split stria vascularis. *c* Representation of the cochlear lateral wall (*Intermed.* intermediate). *Bars*100 μm (**a**), 0.5 mm (**b**)

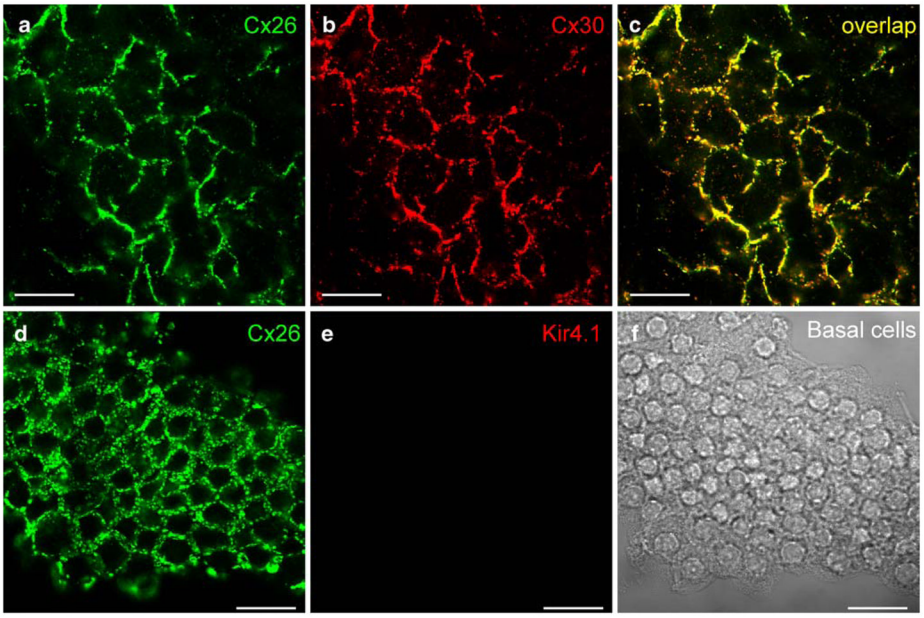

Fig. 2.

Cx26 and Cx30 labeling in the basal cell layer of the rat stria vascularis (SV). **a**, **b** Immunofluorescent images of double-labeling of the SV for Cx26 and Cx30. Confocal images show a honeycomb-like labeling pattern. **c** Merged image of **a**, **b** (*yellow* co-localization). **d**, **e** Double-immunofluorescent labeling of the basal cells for Cx26 and Kir4.1. Cx26 labeling shows a honeycomb-like pattern between the basal cells, but no labeling for Kir4.1 is visible. **f** Nomarski image of fields in **d**, **e**. *Bars*20 μm in (**a**–**c**), 40 μm (**d**–**f**)

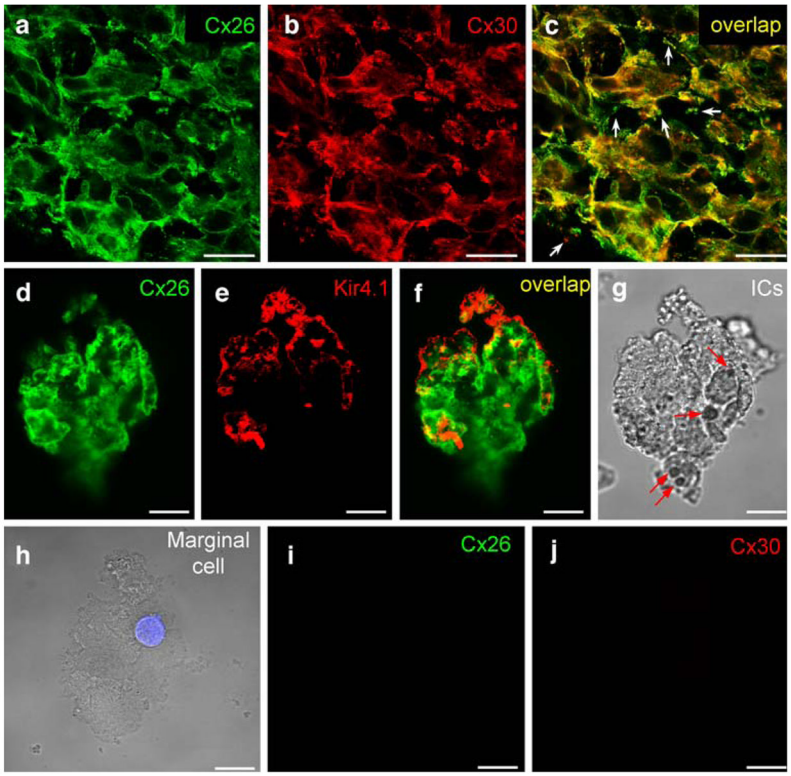

Fig. 3.

Immunofluorescent labeling for Cx26 and Cx30 in the stria intermediate cells and marginal cells. **a**–**c** Double immunofluorescent labeling for Cx26 and Cx30 in the intermediate cell layer of the SV of guinea pig (*yellow* co-localization, *white arrows* in **c** punctate labeling at the cell edge). **d**–**g** Immunofluorescent labeling for Cx26 and Kir4.1 in a dissociated intermediate cell group from rat. Both Cx26 and Kir4.1 show positive labeling (*yellow* co-localization, *arrows* in **g** black pigment granules visible in cytoplasm, *ICs* intermediate cells). **h**–**j** Negative immunofluorescent labeling for Cx26 and Cx30 in a marginal cell. The cell nucleus is revealed by DAPI staining (*blue*). No pigment granules are visible in the cytoplasm. *Bars*20 μm (**a**–**c**), 10 μm (**d**–**j**)

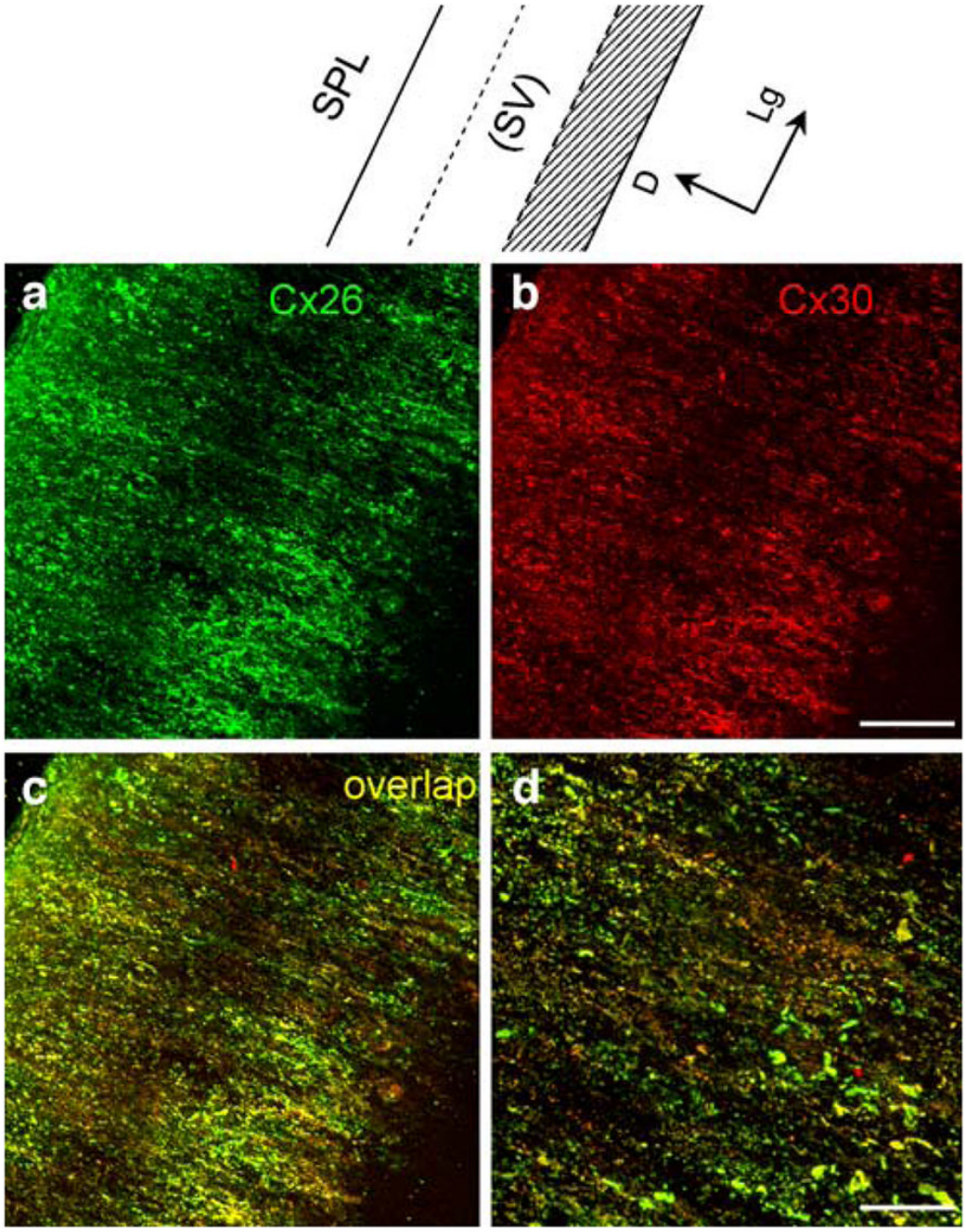

Fig. 4.

Double immunofluorescent labeling of the rat spiral ligament (*SPL*) for Cx26 and Cx30 (*SV* stria vascularis). **a**, **b** Confocal immunofluorescent images for Cx26 and Cx30 labeling. **c** Merged image of **a**, **b** (*yellow* co-localization). **d** Higher magnification image of **c**. Note that the SV had been removed from the SPL before staining. *Top* Representation of the SPL for orientation (*shadowed area* spiral prominence and the inferior region below the spiral prominence, *D* dorsal, *Lg* longitudinal). *Bars* 50 μm (**a**–**c**), 20 μm (**d**)

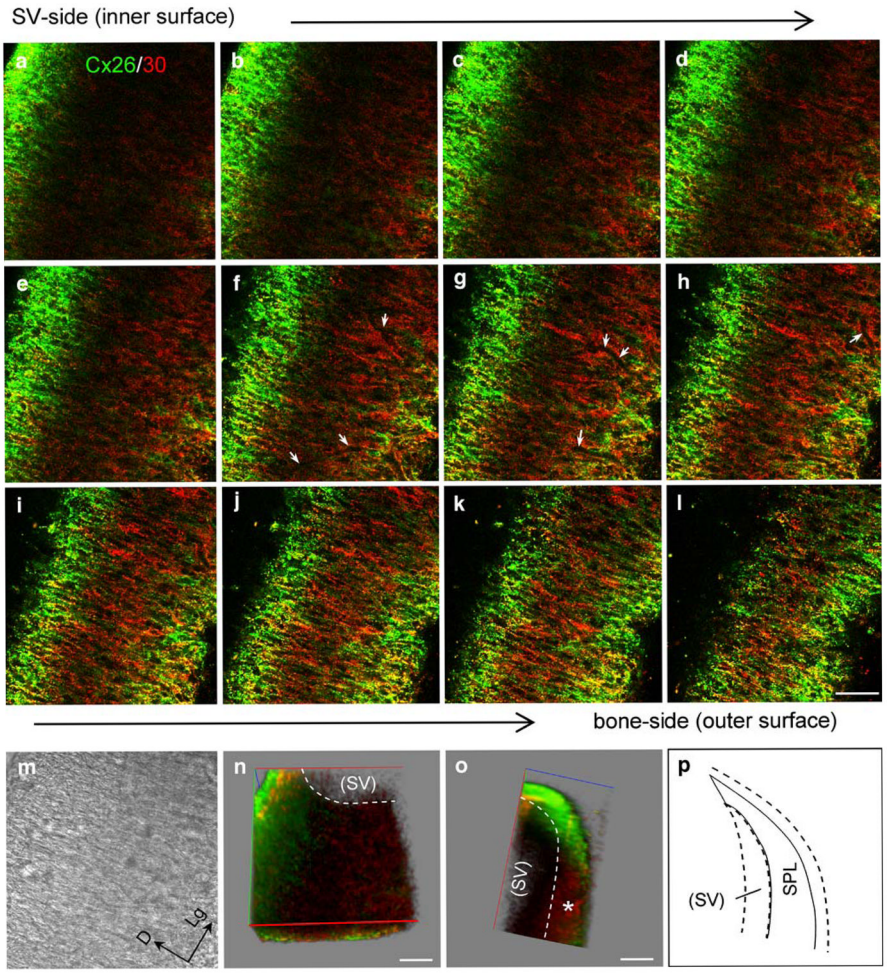

Fig. 5.

Cx26 and Cx30 labeling in serial confocal scanning sections of the separated rat spiral ligament (*SPL*) at the middle turn. **a**–**l** Sections were serially scanned from the inner surface (*SV-side*) of the SPL to its outer surface (*bone-side*) in 3.25-μm steps (*green* Cx26 labeling, *red* Cx30 labeling, *yellow* co-localization, *white arrows* in **f**–**h** "shadows" of blood vessels). **m** Nomarski image of **d** (*D* dorsal, *Lg* longitudinal). **n**, **o** Reconstructed three-dimensional images. *Red*, *green*, and *blue* axes represent the X, Y and Z axes, respectively. **n** View of the X-Y plane from a small angle in the Z axis. Note that the stria vascularis (*SV*) had been removed from the SPL before staining. **o** Orthogonal cross-sectional view at the X-Z plane (*asterisk* region beneath the SV with little Cx26 labeling). *Bars*50 μm. **p** Representation of the orthogonal cross-sectional view at the X-Z plane

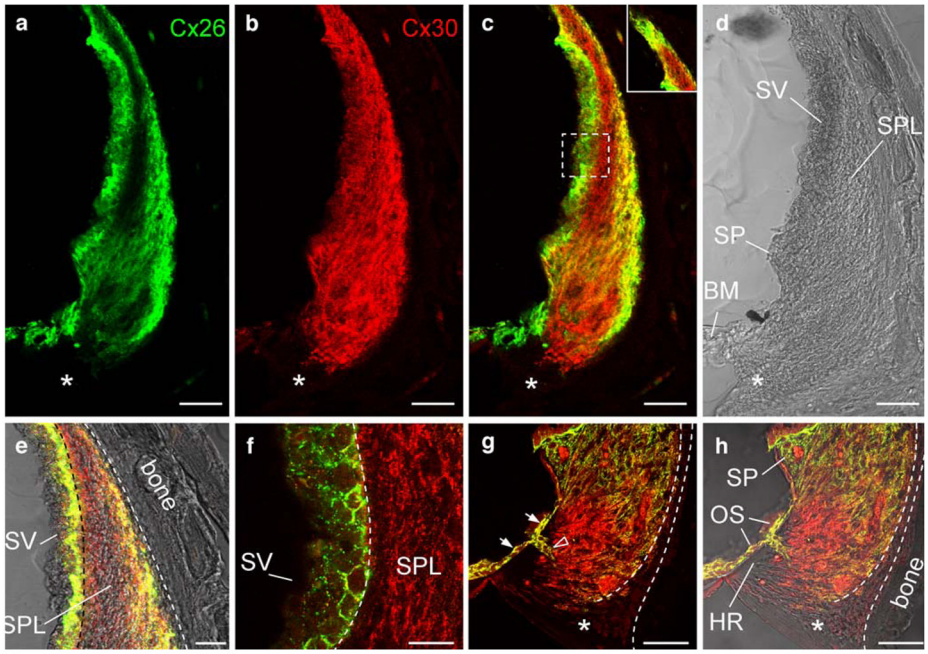

Fig. 6.

Immunofluorescent labeling of the cochlear lateral wall for Cx26 and Cx30 in a midmodiolar section through the rat cochlea. **a**–**d** Orthogonal cross section of the rat cochlear lateral wall in the middle turn through the mid-modiolus (*green* Cx26 labeling, *red* Cx30 labeling, *yellow* co-localization, *asterisks* subcentral region with no Cx26 and 30 labeling). **c** Merged image of immunofluorescent labeling for Cx26 and Cx30. *Inset* Labeling at the apical tip of the SPL. **e** Higher magnification image at the middle region of the SV and SPL. **f** Higher magnification image of the *dashed box* in **c. g**, **h** High magnification images at the inferior region of the SPL. **g** Merged image of immunofluorescent labeling for Cx26 and Cx30 (*white arrows*, *open arrowhead* intense labeling for Cx26 and Cx30 in the outer sulcus cells and their root processes respectively, *OS* outer sulcus cells, *dashed lines* tension fibrocyte area, *asterisks* in **g**, **h** subcentral region, *BM* basilar membrane, *HR* hyaline region, *SP* spiral prominence, *SPL* spiral ligament, *SV* stria vascularis). *Bars* 50 μm (**a**–**d**, **g**, **h**), 25 μm (**e**), 20 μm (**f)**

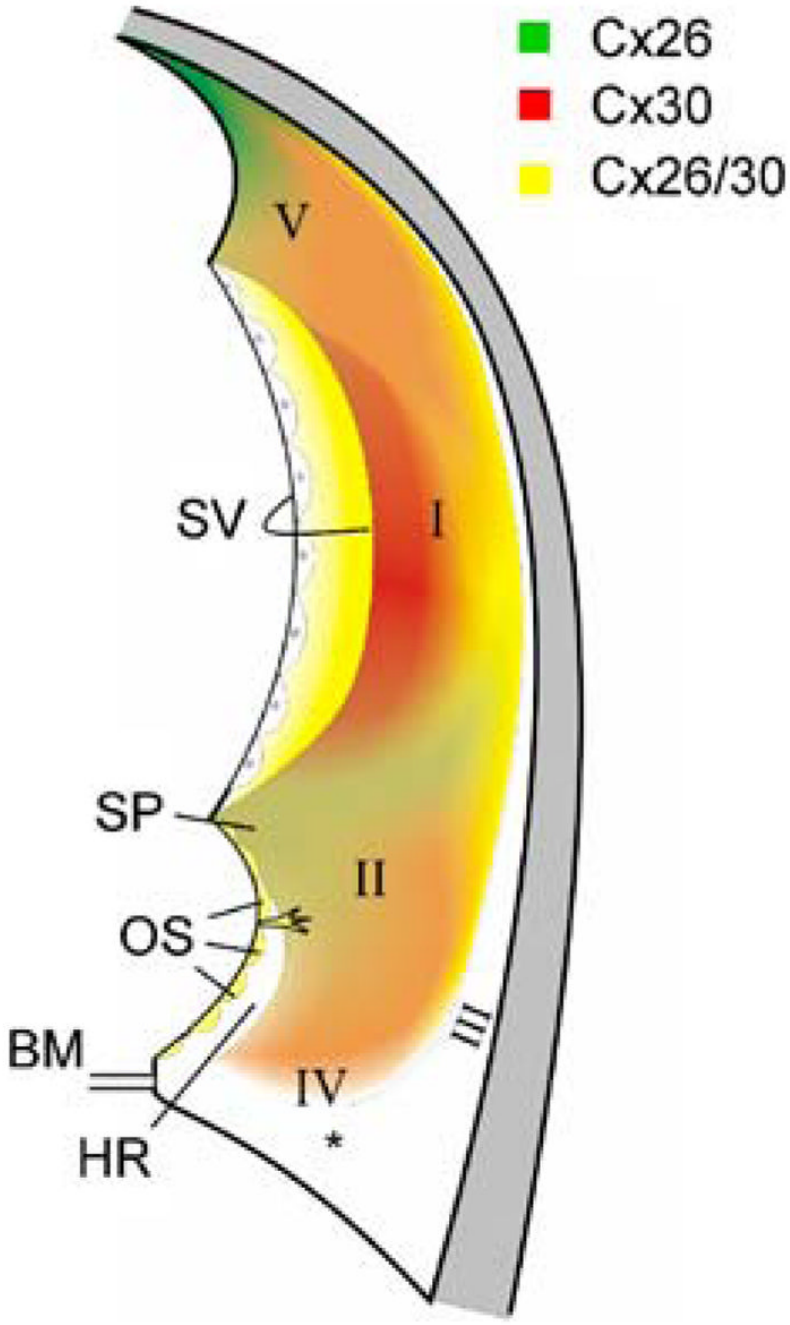

Fig. 7.
Representation of the cellular distributions of Cx26 and Cx30 in the cochlear lateral wall. The approximate location of the different subtypes of fibrocytes in the SPL is indicated (*I–V* fibrocyte subtypes, *asterisk* subcentral region, *BM* basilar membrane, *OS* outer sulcus cell, *HR* hyaline region, *SP* spiral prominence, *SV* stria vascularis)